www.czasopisma.pan.pl PAN POLSKA AKADEMIA NAUK www.journals.pan.pl

Arch. Metall. Mater. **68** (2023), 1, 215-222

DOI: https://doi.org/10.24425/amm.2023.141497

B. WINIARSKA[1*], P. GUZDEK[2], J. KUCIAKOWSKI[3,4], W. TOKARZ[3], M. SIKORA[4], J. PSZCZOŁA[3]

MAGNETOSTRICTIVE FUNCTIONAL MATERIALS OF $Tb_{0.27}Dy_{0.73}(Fe_{1-x}Al_x)_2$ SERIES AS PROSPECTIVE CONSTITUENTS OF MAGNETOELECTRIC COMPOSITES

Structural, magnetic, and magnetostrictive properties of two-sublattice $Tb_{0.27}Dy_{0.73}(Fe_{1-x}Al_x)_2$ polycrystalline intermetallic ferrimagnets (x = 0−0.2 and 1.0) were studied using X-ray powder diffraction, magnetometry, and strain gauge magnetostriction measurements. Temperature dependences of magnetization starting from 80 K were presented, and Curie temperatures were estimated. Coercive force, residual, and saturation magnetizations were determined from the magnetic hysteresis loops at room temperature. Longitudinal, transversal, form and volume magnetostrictions were investigated against the x parameter and the intensity of the magnetic field. The piezomagnetic coefficients were determined and the maximum value at the field below 1 kOe, even enhanced than that in Terfenol-D, was observed for the material $Tb_{0.27}Dy_{0.73}(Fe_{0.9}Al_{0.1})_2$. It means that this compound is promising for use in magnetoelectric composites.

Keywords: intermetallics; magnetization; Terfenol-D; magnetostriction; magnetoelectric composites

1. Introduction

Heavy rare earth (R) − 3d transition metal (M) compounds are typically treated as two-sublattice metallic ferrimagnets [1,2]. Ferrimagnetism of the RM_2-type compounds is a result of a coexistence of the 4f(5d)- and 3d-magnetism [3,4]. In the intermetallic compounds, the $5d^16s^2$ electrons of the rare earth atom are transferred to the band. The electron configuration of the R^{3+} ions residing at the crystal sites is $Xe4f^i5(sp)$, where, i = 8, 9 for Tb, Dy, respectively. The well-localized atomic-like 4f-electrons are shielded from the rest of the lattice by more outer, also atomic-like 5sp-electrons. Therefore direct 4f−4f or 4f−3d exchange interactions are practically absent. It is a quantum-mechanical effect that the 5d(6s) band electrons partially reside at the rare-earth sites. As a result, the 4f−5d(6s)−4f and 4f−5d(6s)−3d exchange interaction paths are essential in the rare earth-transition metal compounds [2,5].

A variety of useful properties of these materials induces permanent scientific and practical interest in the studies. For instance, many R−M ferrimagnets exhibit huge magnetostrictive properties [6]. Extremely high magnetostriction for $TbFe_2$ and $DyFe_2$ compounds was observed at room temperature [7]. Unfortunately, these compounds have significant magnetocrystalline anisotropy, and thus in practical use, they require high values of magnetic field intensity to be fully magnetized. As a result of studies of the $Tb_{1-x}Dy_xFe_2$ series, the existence of large magnetostriction along with reduced magnetocrystalline anisotropy was derived for the $Tb_{0.27}Dy_{0.73}Fe_2$ compound, commercially known as Terfenol-D [7].

Reduced magnetocrystalline anisotropy facilitates the practical use of the Terfenol-D and materials similar to it, and thus induces topical studies of such compounds [6]. Such materials are used in sensors, actuators, ultrasonic transducers, broadband shakers, surgical instruments, hearing aids, accelerometers, proximity sensors, torque sensors, and magnetometers [8-10]. Additionally, they are used as strongly magnetostrictive constituents of composites with piezoceramics or piezopolymers to attain a giant magnetoelectric effect [11-13]. It should be mentioned that magnetoelectric materials have attracted a great deal of attention not only from the perspective of material science but also for their practical applications in transducers, spintronics, information storage, sensors, energy harvesters, and the design of new types of the electronic device [14].

The influence of 3d transition metal sublattice on the crystal, magnetic, and even hyperfine interactions of the R−M intermetallics can be tested by substitution method, i.e. by the gradual

[1] KAZIMIERZ PULASKI UNIVERSITY OF TECHNOLOGY AND HUMANITIES IN RADOM, UL. MALCZEWSKIEGO 29, 26-600 RADOM, POLAND
[2] ŁUKASIEWICZ RESEARCH NETWORK – INSTITUTE OF MICROELECTRONICS AND PHOTONICS, AL. LOTNIKÓW 32/46, 02-668 WARSAW, POLAND
[3] AGH UNIVERSITY OF SCIENCE AND TECHNOLOGY, FACULTY OF PHYSICS AND APPLIED COMPUTER SCIENCE, AL.MICKIEWICZA 30, 30-059 KRAKOW, POLAND
[4] ACADEMIC CENTRE FOR MATERIALS AND NANOTECHNOLOGY AGH, AL.MICKIEWICZA 30, 30-059 KRAKOW, POLAND
* Corresponding author: b.winiarska@uthrad.pl

replacement of the magnetic *M*-atoms by nonmagnetic aluminium ones; examples are given in [15,16]. Consequently, the number of the $4f$–$5d(6s)$–$3d$ exchange interaction paths mentioned above is reduced. Therefore it can be expected that Fe/Al replacements can essentially modify magnetic and particularly magnetostrictive properties of the $Tb_{0.27}Dy_{0.73}Fe_2$ compound in the transition metal sublattice. The literature data related to the intermetallics derived from the starting $Tb_{0.27}Dy_{0.73}Fe_2$ compound by the Fe/Al substitution are rather modest [17-19]. Therefore, it was interesting to systematically test the Fe/Al substitution as a factor modifying the crystal, magnetic, and especially magnetostrictive properties of the $Tb_{0.27}Dy_{0.73}(Fe_{1-x}Al_x)_2$ intermetallic series, for possible application of new materials to design brand new magnetoelectrics. For this purpose, the synthesis, crystallographic studies, magnetic and magnetostrictive measurements against temperature, and magnetic field intensity have been performed for Terfenol-D and its derivative compounds.

2. Experimental

2.1. Synthesis

Polycrystalline samples with stoichiometry $Tb_{0.27}Dy_{0.73}(Fe_{1-x}Al_x)_2$ (x = 0, 0.05, 0.1, 0.15, 0.2, 1) were synthesized by arc melting of the constituent metals Tb (99.9 % purity), Dy (99.9% purity), Fe (99.99% purity) and Al (99.99% purity). The process took place in a high purity argon atmosphere in the furnace with a non-contact arc ignition described elsewhere [20]. The synthesized samples were then annealed in a vacuum at 850°C for one hour and then cooled down within the furnace.

2.2. Magnetic measurements

Magnetization measurements in the temperature range of 80 to 300 K were performed under the magnetic field 6500 Oe using the vibrating sample magnetometer (VSM). Fine powder samples were tightly pressed in a sphere inside of a diamagnetic enclosure. Dimensions of the powder crystallites with a variety of irregular shapes tested by scanning electron microscope can be ascribed to the length range (1-10) μm.

In the case of high-temperature measurements, another vibrating sample magnetometer equipped with an oven has been used. Bulk samples were heated with a flow of Ar gas. Small samples were cut out from larger ingots and installed in the magnetometer in such a way that the demagnetization effects were minimized.

2.3. Magnetostrictive measurements

The magnetostriction was measured at room temperature using a standard strain gauge measuring system. After polishing and cleaning the surfaces of the slice-type sample (in an oval shape and a thickness of approx. 1 mm), a flexible strain gauge was fixed to the surface using cyanoacrylic glue. The samples with the strain gauge were placed parallel or perpendicular to the steady magnetic field. The strain gauge attached to the sample was connected as the branch of a Wheatstone bridge, which was made up of the same type of strain gauges. The Wheatstone bridge was electrically excited with a strain gauge measuring system. The rated resolution in measuring the magnetostriction was better than 2 ppm.

3. Results and discussion

3.1. Crystal structure

Good quality powder diffractograms, measured at room temperature using a conventional *X*-ray apparatus with a Mo lamp, presented for the synthesized materials (Fig. 1), were analysed using a Rietveld-type method considering $K_{\alpha1}$ and $K_{\alpha2}$ lines [21,22]. It should be noted that at higher 2θ values, a splitting of the peaks due to the $K_{\alpha1}$ and $K_{\alpha2}$ lines can be observed.

The angular split $\Delta\theta$ depends on the angle θ, and its absolute value increases with this angle. This dependence can be described by the formula [23]

$$\Delta\theta = -\frac{2 \cdot d_{hkl}}{\lambda} \operatorname{tg}\theta \sin\theta \tag{1}$$

Analysis of the diffractograms revealed a single-phase composition for all compounds. The crystal phases of the materials stabilized in a face-centered cubic Laves $Fd\bar{3}m$, $MgCu_2$-type structure. The *C*15 Laves phase has been described in detail elsewhere [24] and its unit cell for $x = 0$ and $x = 1$ are visualized in Fig. 1. In the presented diffractograms, experimental data are marked by red points, black lines show fitted diffractograms, and additionally, differential patterns in blue are situated below corresponding diffractograms. Moreover, positions of the diffraction reflections are indicated by green markers corresponding to the suitable Miller coefficients presented at the peaks.

The determined lattice parameter a equals 7.339(2) Å for the initial $Tb_{0.27}Dy_{0.73}Fe_2$ compound (Fig. 2) and increases linearly across the series up to 7.435(2) Å for the $Tb_{0.27}Dy_{0.73}(Fe_{0.8}Al_{0.2})_2$ compound (TABLE 1). The lattice parameter is expressed numerically with the formula $a(x) = (0.474x + 7.340)$ Å. In this case, Vegard's rule is obeyed, because Fe atoms of a smaller atomic radius (r_{Fe} = 1.72 Å) were substituted by the Al atoms of the radius r_{Al} = 1.82 Å [25].

The obtained data (black points) coincide satisfactorily with those known from the literature (open circles) for the $Tb_{0.27}Dy_{0.73}(Fe_{1-x}Al_x)_2$ series [17,18] and the $Tb_{0.27}Dy_{0.73}Fe_2$ compound [9,26].

Moreover, in Fig. 2 the inset shows the experimental $a(x)$ dependence, including the a value for the $Tb_{0.27}Dy_{0.73}Al_2$ compound (7.855 Å). A linear tendency can be carefully concluded.

In Fig. 2, the average number n of $3d$ electrons calculated per site of the $3d$ transition metal sublattice is presented in

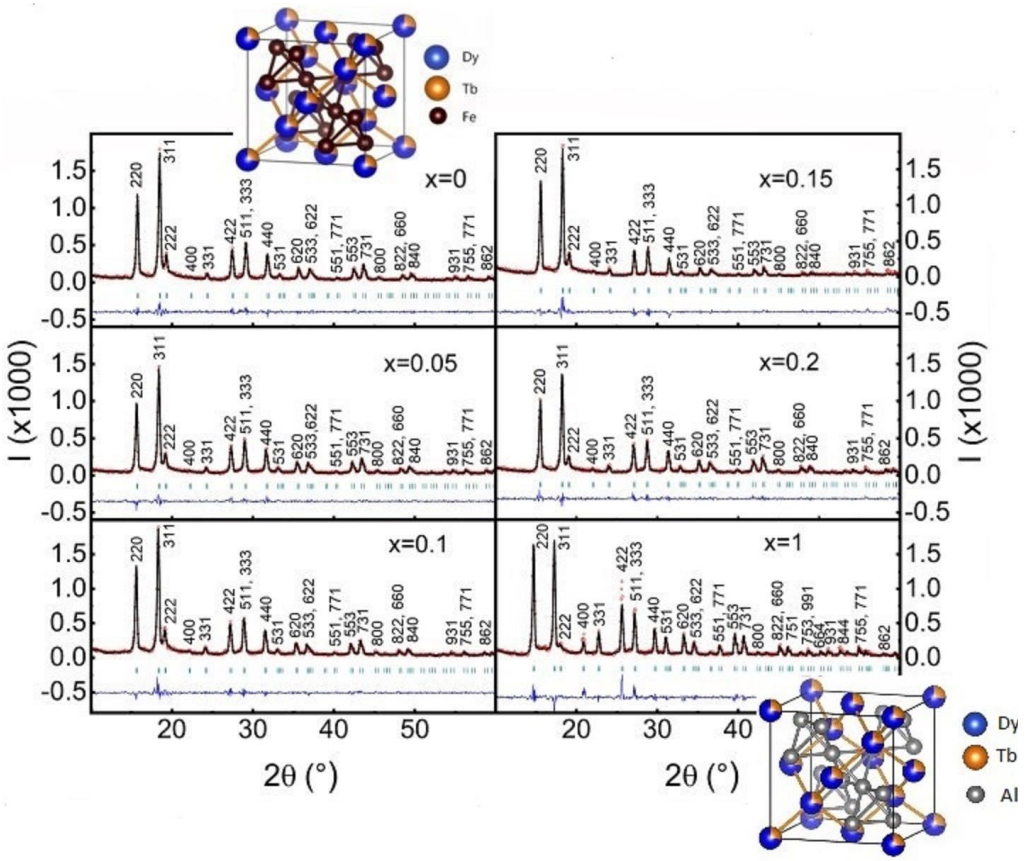

Fig. 1. X-ray powder diffraction patterns I(2θ) observed for the $Tb_{0.27}Dy_{0.73}(Fe_{1-x}Al_x)_2$ intermetallics (300 K). Red points mark experimental data, fitted diffractograms are shown by black lines, and differential patterns in blue are added below each diffractogram. Positions of the diffraction reflexes are indicated by green markers corresponding to the suitable Miller coefficients presented above the peaks. The *x*-parameters are added for each diffractogram. $MgCu_2$ crystal structure for $x = 0$ and $x = 1$ visualised using VESTA software

TABLE 1

Crystal structure, magnetization and magnetostriction parameters for $Tb_{0.27}Dy_{0.73}(Fe_{1x}Al_x)_2$

x	*a* Å	d_{rtg} g/cm^3	M_s μ_B/f.u.	M_r μ_B/f.u.	H_c kOe	E_{hy} μ_BkOe/f.u.	T_C K	*L* 10^{-6}	*k*	*m*
0.00	7.339 7.336 [10] 7.330 [22] 7.345 [23] 7.330 [24]	9.18	3.143	0.557	0.370	6.14	637 650 [27] 660 [18]	1513.3	1.88	1.58
0.05	7.363 7.355 [22]	8.99	3.088	0.551	0.311	6.00	588	1309.2	1.53	1.85
0.10	7.390 7.382 [22] 7.385 [23]	8.80	2.987	0.423	0.244	4.10	530 540 [18]	981.6	0.75	1.71
0.15	7.408 7.410 [22]	8.64	3.140	0.247	0.181	1.59	482	601.2	0.76	1.76
0.20	7.435 7.432 [22] 7.430 [23]	8.46	2.390	0.224	0.119	1.35	410 395 [18]	237.9	1.04	2.65
1.00	7.855	5.91	0.388	0.025	0.115	0.18	75 [19]*	8.5	0.53	1.73

* for $(Tb_{0.25}Dy_{0.75}Al_2)$ compound

the top axis. The number *n* is calculated following formula $n = 6(1 - x)$, where six is the number of 3*d* electrons of the iron atom. The density for Terfenol-D derived from *X*-ray data equals $d_{rtg} = 9.18$ g/cm^3, which is close to the literature value of this parameter 9.2 g/cm^3 [27]. The densities across the series of compounds are presented in TABLE 1.

It can be added that the unit cell contains 24 atoms in all. The cubic phase has two non-equivalent crystal sites, *R* atoms

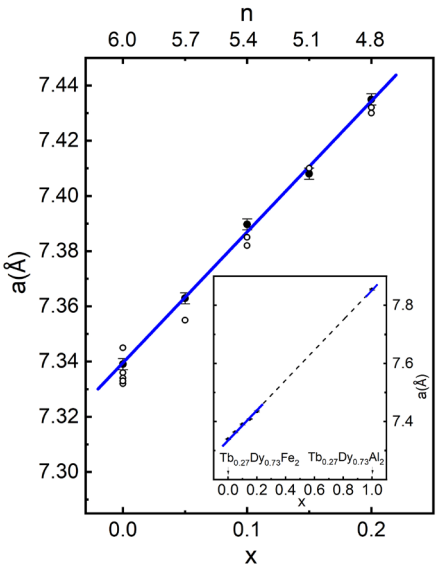

Fig. 2. The unit cell parameter a (the inset with $x = 1$ point) against the composition parameter x (or number n). Open points after [11,17,18,26]

occupy the 8a sites, and M-atoms occupy the 16d sites. Each R-ion has 12 M-atoms in the nearest neighbour shell (radius $0.415a$) and 4 slightly more distant R-ions in the next-nearest neighbour shell (radius $0.433a$). Each M-atom has six M-atoms in the nearest neighbour shell (radius $0.354a$) and six R-ions (at $0.415a$) as next-nearest neighbours.

3.2. Magnetization

There are many studies of the magnetic properties of Terfenol-D at room temperature, but studies of the magnetic properties of this material as functions of temperature are somewhat limited. Thus, it was interesting to study magnetization against temperature for this compound and its derivative compounds introduced by Fe/Al substitution.

A consistency of experimental curves in a standard room temperature range is limited approximately by experimental errors not bigger than 3%.

Fig. 3 presents $M(T)$ (at 6500 Oe) magnetizations observed for the intermetallic system $Tb_{0.27}Dy_{0.73}(Fe_{1-x}Al_x)_2$ (x = 0–0.2, 1.0). Temperatures T_C estimated from the dM/dT derivatives are contained in TABLE 1. The literature T_C – values are also added [27]. The Curie temperature decreases almost linearly with the aluminium content x in the x = 0–0.2 substitution range. The decrease of T_C values is significant in this case.

For all studied compounds, magnetic isothermal loops $M(H)$ were gathered at room temperature. It should be mentioned that the magnetization values taken from the hysteresis loop fit well with the corresponding values from the graphs of the temperature dependences of the magnetization.

Visible in Fig. 3 reference lines (M = 0) throw up the asymptotic, not-sharp character of the gradual decrease of the magnetization value with growing temperature in the paramagnetic regime ($T > T_C$).

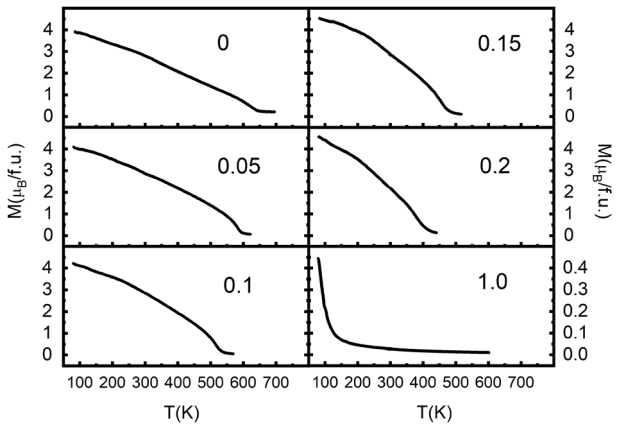

Fig. 3. The magnetizations $M(T)$ measured at 6.5 kOe for the $Tb_{0.27}Dy_{0.73}(Fe_{1-x}Al_x)_2$ series

For x = 1, even in T = 600 K (far above estimated T_C for this compound) one can observe a very small but still non-zero value of the magnetic moment ($M(600\,K)_{x=1} \cong 0.01\mu_B$/f.u.). This is related to the Disorder-Broaden First Order Transition described in [30], observed among others, for anisotropic RM_2-type compounds. Magnetic phase transition is not of sharp character in this case.

For studied $Tb_{0.27}Dy_{0.73}(Fe_{1-x}Al_x)_2$ series existence of two sublattices introduce some inhomogeneity affecting the anomalous broadening of the magnetic phase transition. Whilst, for the compound $Tb_{0.27}Dy_{0.73}Al_2$, the sublattice M does not contribute to the magnetization, however, dilutes the crystallographic lattice introducing additional inhomogeneity.

It should not be forgotten that in a crystal, the direction of the magnetic moment strongly depends on the interaction with its local neighbors (spin-orbit coupling). In an anisotropic crystal, this interaction depends also on the crystallographic axis, Such inhomogeneous distribution of moments favors the formation of small areas that are assemblies of magnetic moments (more difficult to demagnetize) and areas in which the magnetic moments are further apart (easier to demagnetize). It is easy to guess that in different areas the moments are ordered and disordered at different temperatures, which on average affects the broadening of "point" Curie into the "band/range" Curie. Thus, the Ferromagnetic-Paramagnetic phase transition process runs much slower and in a wider temperature range than in the ideally isotropic material.

There is ambiguity in defining the phase transition temperature, indeed. The most common is the criterion of two points between which the most abrupt change of order occurs and sets the temperature T_C as the midpoint between them. The temperature T_C for the studied compounds was determined for the most rapid change in the degree of order. But above T_C there is still coexistence of two magnetic phases (F and P), and ferromagnetic phase content gradually and relatively slowly decreases with temperature.

Fig. 4 shows the sigmoidal hysteresis loops, i.e., the magnetization M against the magnetic field strength H observed at room temperature for these intermetallics.

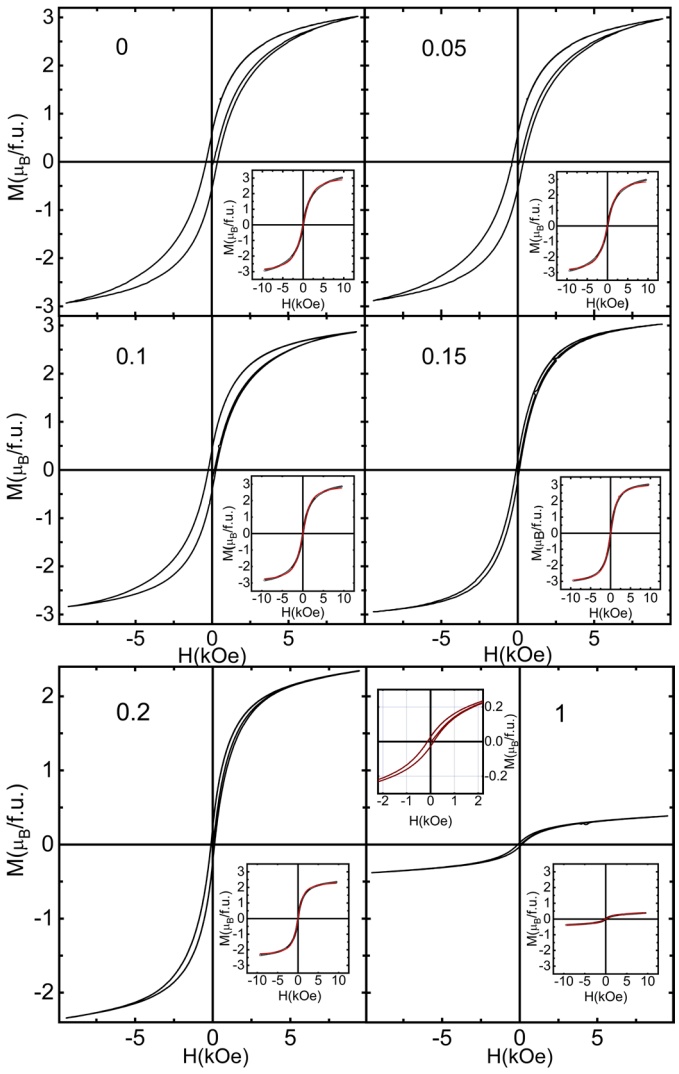

Fig. 4. The $M(H)$ binal sigmoidal magnetic hysteresis loops for $Tb_{0.27}Dy_{0.73}(Fe_{1-x}Al_x)_2$ series (300 K). The x-parameters added to each plot. The average $M(H)$ dependencies with the corresponding to them Langevin curves are presented in insets. Plots for $x = 0.2$ and $x = 1$ on a slightly enlarged scale. Additional inset for $x = 1$ presents enlarged hysteresis portion

From the $M(H)$ hysteresis loops, it follows that the growing x-parameter, in the range of $x = 0{-}0.02$, facilitates magnetic saturation.

It should be noted that for the $Tb_{0.27}Dy_{0.73}Al_2$ compound, with complete substituted Fe atoms by Al atoms, far above its Curie temperature (75 K [19] < T_C < 80 K – the lower limit of the measurement range), the hysteresis loop of negligible but noticeable ferromagnetic nature is observed. This should be explained by the aforementioned disorder-broaden F-P phase transition.

Parameters of interest that characterize the hysteresis loop include the coercive force H_c, the residual magnetization M_r (or the residual magnetic induction B_r), and saturation magnetization M_s (TABLE 1). Based on Fig. 5 and data contained in the table, it can be concluded that the M_r and H_c parameters actively reduce across the series.

Since the M_r and the H_c parameters rather don't reach very high values, thus the studied intermetallics can be treated as materials with small energy loss per cycle which is approximated by the formula [28,29]

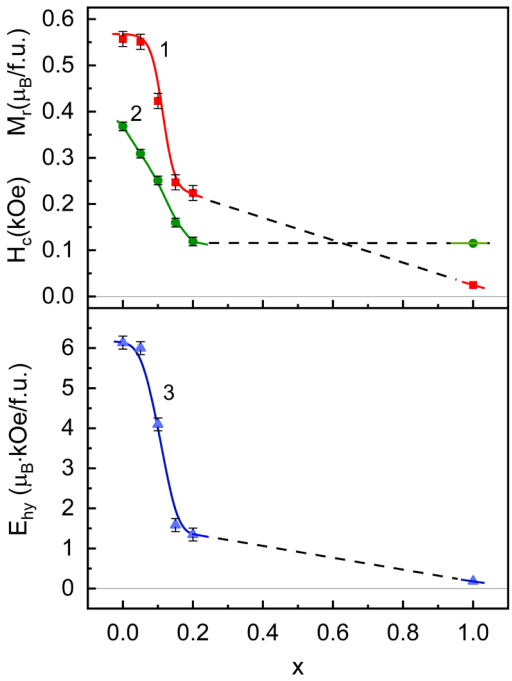

Fig. 5. The residual magnetization M_r (curve 1), coercive force H_c (curve 2), and energy loss E_{hy} (curve 3) for the $Tb_{0.27}Dy_{0.73}(Fe_{1-x}Al_x)_2$ series (300 K)

$$E_{hy} = \mu_0 \oint_{loop} H dM \tag{2}$$

This hysteresis energy loss per cycle E_{hy} is proportional to the area of the $M(H)$ loop and equals 0.569, 0.556, 0.380, 0.147, 0.125 and 0.016, all × 10^{-23} J/f.u., for $x = 0$,0.05,0.1,0.15,0.2 and 1.0, correspondingly. This is inconsiderable energy loss and additionally, it strongly falls in the $x = 0{-}0.2$ region with the Fe/Al replacing. The $E_{hy}(x)$ function changes as does the remanence $M_r(x)$ function and the coercivity $H_c(x)$ (TABLE 1, Fig. 5).

Concerning the existence of magnetic loops with the residual magnetization M_r and the coercive force H_c, it can be concluded that the $Tb_{0.27}Dy_{0.73}(Fe_{1-x}Al_x)_2$ compounds are typical metallic ferrimagnets.

The anhysteretic magnetization curve obtained from the half sum of the hysteresis loop branches, namely $M(H) = 0.5[M(H)_{upper} + M(H)_{lower}]$ can be described well by the Langevin function expressed by the formula:

$$M(H) = M_s \left[\coth \alpha H - \frac{1}{\alpha H} \right] + \beta \tag{3}$$

with the fitted M_s, α, and β parameters. The α parameter equals 1.14, 1.15, 1.35, 1.60, 1.88 and 1.16 kOe^{-1} for $x = 0$, 0.05, 0.1, 0.15, 0.2 and 1, correspondingly. The parameter β (μ_B/f.u.) approaches small values between 0.02 for $x = 0$ and 0 for $x = 1$.

The anhysteretic $M(H)$ dependences (open points) along with the corresponding Langevin fitted curves (in red) are presented in Fig. 4 at the bottom right inset for each x-value compound. A satisfactory coincidence between these curves has been

obtained. The fitted saturation magnetic moments M_s (μ_B/f.u.) for the compounds of the series are presented in TABLE 1.

3.3. Magnetostriction

The term magnetostriction $\lambda = \Delta l/l$ refers to the relative change in the dimension l of the sample magnetized in the external magnetic field H.

Whereby, longitudinal magnetostriction $\lambda_{\parallel}$ means the result of the measurement of the linear dimension taken along the direction of the field ($l \parallel H$), and transversal magnetostriction $\lambda_{\perp}$ is measured perpendicularly to the field ($l \perp H$). Both $\lambda_{\parallel}$ and $\lambda_{\perp}$were determined experimentally, while both form λ_{τ} and volume λ_V magnetostrictions were computed numerically on their basis, according to the following formulae:

$$\lambda_{\tau} = \lambda_{\parallel} - \lambda_{\perp} \tag{4}$$

$$\lambda_V = \lambda_{\parallel} + 2\lambda_{\perp} \tag{5}$$

Fig. 6 shows the magnetic field dependences of the longitudinal $\lambda_{\parallel}$, transversal $\lambda_{\perp}$, form λ_{τ} (sometimes called anisotropic magnetostriction) and volume λ_V magnetostrictions. Analogously, as for the hysteresis loops, the growing x-parameter facilitates the saturation of the longitudinal $\lambda_{\parallel}$, transversal $\lambda_{\perp}$, and form λ_{τ} magnetostrictions. Additionally, the growing x-parameter shifts sequentially these $\lambda(H)$ dependences to the zero-value axis. This result is similar to that presented elsewhere [18]. Nevertheless, even at x = 0.2, the absolute values of the magnetostrictions approach quite large values. The lines in Fig. 6 are fitted by the so-called Hill functions, expressed for form magnetostriction λ_{τ} by the formula:

$$\lambda_{\tau}(H) = L\frac{H^m}{k^m + H^m} \times 10^{-6} \tag{6}$$

The parameters L, k, m for the form magnetostriction are contained in TABLE 1, and H is expressed in units of kOe. Based on the dependences $\lambda_{\tau}(H)$, it can be seen that the magnetostriction for the $Tb_{0.27}Dy_{0.73}(Fe_{0.9}Al_{0.1})_2$ compound saturates more easily than for that one observed for the starting compound of the series (x = 0). It can be added that the volume magnetostrictions present regular but non-typical dependences against the magnetic field intensity.

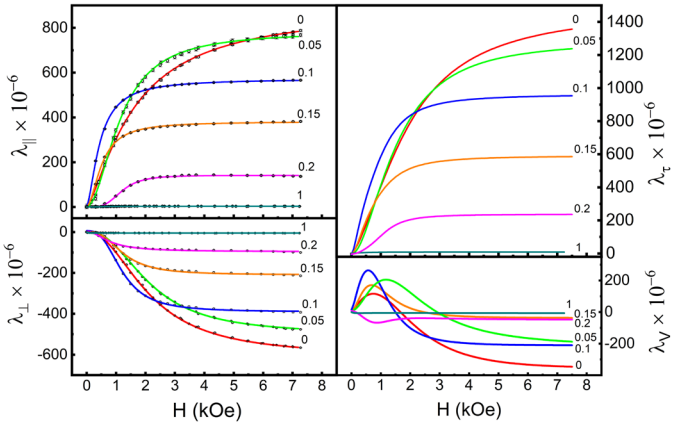

Fig. 6. The longitudinal $\lambda_{\parallel}$, transversal $\lambda_{\perp}$, form λ_{τ}, and volume λ_V magnetostrictions as functions of the steady magnetic field H for the $Tb_{0.27}Dy_{0.73}(Fe_{1-x}Al_x)_2$ series (300 K). The x-parameters added to curves fitted to experimental points

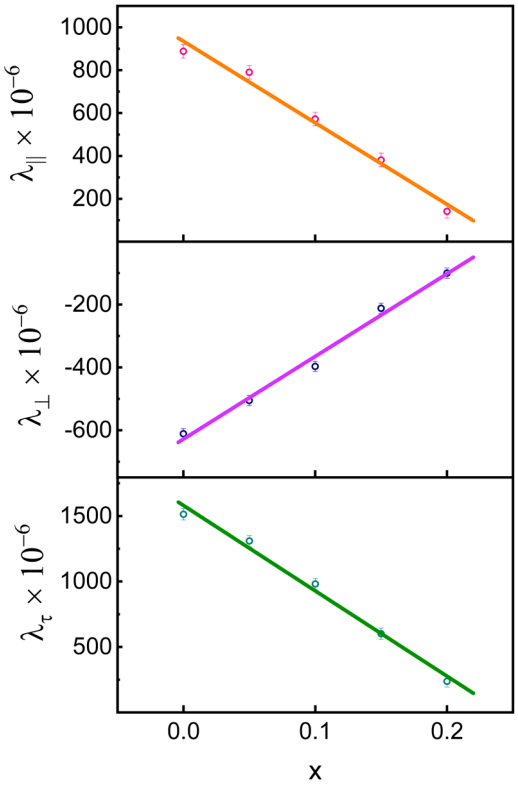

Fig. 7. The magnetostrictions $\lambda_{\parallel}$, $\lambda_{\perp}$ and λ_{τ} (at 6.5 kOe) vs. the x parameter

It is interesting to relate magnetostriction values to the parameter x, which is correlated with the number of iron magnetic moments per unit cell. One should keep in mind that increasing x value means decreasing the iron content. The determined linear correlations, for the range x = 0–0.2, are presented in Fig. 7. These experimental relationships are described by the following formulae:

$$\lambda_{\parallel}(x) = -380x + 935 \tag{7}$$

$$\lambda_{\perp}(x) = 2630x - 628 \tag{8}$$

$$\lambda_{\tau}(x) = -6518x + 1580 \tag{9}$$

Fig. 8 presents the so-called piezomagnetic coefficients $d\lambda\tau(H)/dH$ vs. H, calculated from magnetic field dependences of the form magnetostriction [8]. Numbers with arrows correspond to x-values, and numbers in brackets are coordinates of the maxima of each curve. Practically, the maximum values of $d\lambda\tau(H)/dH$ coefficients are located above H = 0.3 kOe and below H = 0.8 kOe. Since the piezomagnetic coefficient has the highest value for the $Tb_{0.27}Dy_{0.73}(Fe_{0.9}Al_{0.1})_2$ compound, this material can be successfully used in magnetoelectric composites. It can also be seen in Fig. 8 that $d\lambda\tau/dH$ parameter above H = 6 kOe, i.e., the slope rates of $\lambda_{\tau}(H)$ dependences decrease

systematically with x. Moreover, $d\lambda\tau/dH$ parameters for $x = 0.1$, 0.15 and 0.20 in this H-area are close to zero. It should be noted that the isothermal volume magnetostriction λ_V, the isothermal $d\lambda\tau/dH$ parameter, and the isothermal magnetic susceptibility M/H obtained for the averaged loop magnetizations (not presented here), all as functions of H, change to some extent similarly.

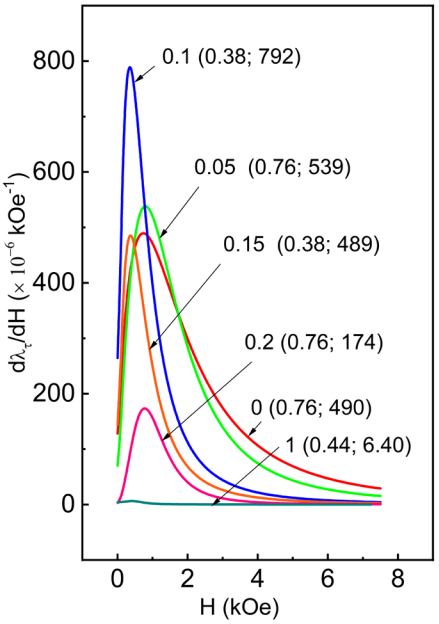

Fig. 8. The piezomagnetic coefficient $(d\lambda\tau(H))/dH$ vs. magnetic field intensity H for the $Tb_{0.27}Dy_{0.73}(Fe_{1-x}Al_x)_2$ series (300 K). The x-parameters added. Numbers in bracket are coordinates of maximal points

5. Conclusion

Synthesis, crystal structure, magnetic, and magnetostrictive properties were studied for the $Tb_{0.27}Dy_{0.73}(Fe_{1-x}Al_x)_2$ intermetallics. The Fe/Al substitution in this series magnetically dilutes the 3*d* transition metal sublattice, reduces the average number of 3*d* electrons with the x-parameter, and thus modifies 3*d* bands as well as crystal and magnetic properties. The lattice parameter grows up with x, but the remaining parameters mostly reduce as a result of Fe/Al substitution.

In the *R*−*M* intermetallics, the rare-earth ions correspond for the giant magnetostriction, whereas the transition metal atoms provide the magnetic order of the system far above the room temperature [6].

Principally, the *Fe*/*Al* replacing reduces the probability $12(1-x)/12$ of the *R*−*M* exchange interactions of the 4*f*−5*d*(6*s*)−3*d* type and thus reduces all magnetic properties and especially reduces magnetostriction by approximately linear manner. For this reason, the magnetic dilution of the iron sublattice reduces the Curie temperature as well as the parameters of the hysteresis loops.

The longitudinal, transversal, and form magnetostrictions reduce their absolute values with the aluminium content increase compared to the starting compound. Despite this, relatively high magnetostrictions are still observed for all tested compounds. Moreover, the growing x parameter facilitates the saturation of all these magnetostrictions ($x = 0-0.2$). Whereby, the most favorable saturation rate is exhibited by compound $Tb_{0.27}Dy_{0.73}(Fe_{0.9}Al_{0.1})_2$, which means that it can be used in the applications realized in lower magnetic fields than Terfenol-D.

Complete replacement of the iron atoms with aluminium ones reduces the magnetostriction coefficients to low values of a few ppm. It should be mentioned that the anomalous results were obtained for $x = 1$. Namely, both the magnetization hysteresis and the magnetostriction curve for this intermetallic show to some extent the course characteristic for ferromagnetic materials, although the measurements were carried out at room temperature, in which this compound should behave like a paramagnet. This anomaly can be understood with help of the theory of Disorder-Broaden First Order Phase Transition. [30]. In the case of the $Tb_{0.27}Dy_{0.73}Al_2$ compound, the disorder (inhomogeneity) results both from its magnetocrystalline anisotropy and the presence of the non-magnetic sublattice *M*.

Since the piezomagnetic coefficients, with their high maxima, are observed at low magnetic field intensities, these materials can be treated as functional constituents of magnetoelectric composites. All these compounds possess relatively large magnetostrictions and significant piezomagnetic coefficients, thus they may be treated as potential materials for applications in the area of sensors, actuators, ultrasonic transducers, and magnetoelectrics. And here again, the most advantageous seems to be compound $Tb_{0.27}Dy_{0.73}(Fe_{0.9}Al_{0.1})_2$, its maximum of the piezomagnetic coefficient is much higher than for Terfenol-D, and also occurs at a much lower value of the magnetic field than for the starting material of the studied series.

Acknowledgements

Dr. D. Tyrała is acknowledged for the scanning electron microscope test of samples. The work has been partly supported by the EU Human Capital Operation Program, Polish Project No. POKL.04.0101-00-434/08-00, by AGH University, project no 11.11.220.01 and by the Polish Ministry of Science and Higher Education from the budget for science in the years 2013-2015, project No. IP2012 029772.

REFERENCES

[1] K.N.R. Taylor, Intermetallic rare-earth compounds Adv. Phys. **20** 551-660 (1971).
DOI: https://doi.org/10.1080/0001-873(71)00101311

[2] K.H.J. Buschow, in: E.P. Wohlfarth (Ed.), Ferromagnetic Materials **1**, North-Holland Publishing Company, Amsterdam (1980).

[3] I.A. Campbell, Indirect exchange for rare earths in metals, J. Phys. F: Metal Phys. **2** L47-L50 (1972).
DOI: https://doi.org/10.1088/0305-4608/2/2/004

[4] B. Gicala, J. Pszczoła, Z. Kucharski, J. Suwalski, Two Slater-Pauling dependences for Dy-3d metal compounds, Phys. Lett. A **185**, 491-494 (1994).
DOI: https://doi.org/10.1016/0375-9601(94)91131-2

[5] S. Legvold, in: E.P. Wohlfarth (Ed.), Ferromagnetic Materials **1**, North-Holland Publishing Company, Amsterdam (1980).

[6] G. Engdahl (Ed.), Handbook of Giant Magnetostrictive Materials, Academic Press, New York (2000).

[7] A.E. Clark, in: E.P. Wohlfarth (Ed.), Ferromagnetic Materials **1**, North-Holland Publishing Company, Amsterdam (1980).

[8] H. Cao, N. Zhang, J. Wei, Doping effect on crystal structure of $BaTiO_3$ and magnetoelectric coupling of layered composites $Tb_{1-x}Dy_xFe_{2-y}$–$BaTi_{0.99}M_{0.01}O_{3+\delta}$, J. Alloys Compd. **472**, 257-261 (2009). DOI: https://doi.org/10.1016/j.jallcom.2008.04.060

[9] P. Record, C. Popov, J. Fletcher, E. Abraham, Z. Huang, H. Chang, R.W. Whatmore, Direct and converse magnetoelectric effect in laminate bonded Terfenol-D-PZT composites, Sens. Actuators B-Chem **126**, 344-349 (2007).
DOI: https://doi.org/10.1016/j.snb.2007.05.047

[10] P. Guzdek, W. Grzesiak, K. Witek, K. Zaraska, B. Winiarska, Liniowy aktuator magnetoelektryczny, Przegląd Elektrotechniczny **8**, 55-58 (2018). DOI: https://doi.org/10.15199/48.2018.08.15

[11] M. Szklarska-Łukasik, P. Guzdek, M. Dudek, A. Pawlaczyk, J. Chmist, W. Dorowski, J. Pszczoła, Magnetoelectric properties of $Tb_{0.27-x}Dy_{0.73-y}Y_{x+y}Fe_2$/PVDF composites, J. Alloys Compd. **549**, 276-282 (2013).
DOI: https://doi.org/10.1016/j.jallcom.2012.08.093

[12] C.W. Nan, M.I. Bichurin, S. Dong, D. Viehland, G. Srinivasan, Multiferroic magnetoelectric composites: Historical perspective, status, and future directions, J. Appl. Phys. **103**, 031101 (2008).
DOI: https://doi.org/10.1063/1.2836410

[13] P. Guzdek, M. Wzorek, Magnetoelectric properties in bulk and layered composites, Microelectron. Int. **32**, 110-114 (2015).
DOI: https://doi.org/10.1108/MI-01-2015-0012

[14] J. Ma, J. Hu, Z. Li, C.W. Nan, Recent Progress in Multiferroic Magnetoelectric Composites: from Bulk to Thin Films, Adv. Mater. **23**, 1062-1087 (2011).
DOI: https://doi.org/10.1002/adma.201003636

[15] J. Pszczoła, B. Gicala, J. Suwalski, ^{57}Fe Slater-Pauling dependence in the $Dy(Fe_{1-x}Al_x)_2$ intermetallic system, J. Alloys Compd. **274**, 47-54 (1998).
DOI: https://doi.org/10.1016/S0925-8388(98)00562-3

[16] J. Pszczoła, P. Stoch, J. Suwalski, J. Żukrowski, Mössbauer effect studies of $Dy[(Fe_{0.7}Co_{0.3})_{1-x}Al_x]_2$ and $Dy[(Fe_{0.4}Co_{0.6})_{1-x}Al_x]_2$ compounds, J. Alloys Compd. **364**, 29-36 (2004).
DOI: https://doi.org/10.1016/S0925-8388(03)00549-8

[17] X. Zheng, P. Zhang, D. Fan, F. Li, Y. Hao, Sci China Ser G: Structure, spin reorientation and Mössbauer effect studies of $Tb_{0.3}Dy_{0.7}(Fe_{1-x}Al_x)_{1.95}$ alloys, Phy. & Ast. **49**, 149-157 (2006).
DOI: https://doi.org/10.1007/s11433-006-0149-5

[18] H. Guo, H. Yang, B. Schen, L. Yang, R. Li, Structural, magnetic and magnetostrictive studies of $Tb_{0.27}Dy_{0.73}(Fe_{1-xAlx)2}$, J. Alloys Compd. **190**, 255-258 (1993).
DOI: https://doi.org/10.1016/0925-8388(93)90407-E

[19] M. Khan, A.K. Pathak, Y. Mudryk, K.A. Gschneidner, Jr., V.K. Pecharsky Anisotropy induced anomalies in $Dy_{1-x}Tb_xAl_2$, J. Mater. Chem. C **5**, 896-901 (2017).
DOI: https://doi.org/10.1039/C6TC05384J

[20] M. Onak, J. Pszczoła, An arc melting system with a non-contact ignition, Phys. Econ. **2**, 27-41 (2018).
DOI: https://doi.org/10.7862/rf.2018.pfe.3

[21] H.M. Rietveld, A profile refinement method for nuclear and magnetic structures, J. Appl. Cryst. **2**, 65-71 (1969).
DOI: https://doi.org/10.1107/s0021889869006558

[22] J. Rodriguez-Carvajal, Recent advances in magnetic structure determination by neutron powder diffraction, Physica B **192**, 55-69 (1993).
DOI: https://doi.org/10.1016/0921-4526(93)90108-I

[23] J. Pszczoła, A. Feret, B. Winiarska, L. Dąbrowski, J. Suwalski, Mössbauer effect studies of $Dy[(Fe_{0.7}Co_{0.3})_{1-x}Al_x]_2$ intermetallics, J. Alloys and Compounds **299**, 59-67 (2000).
DOI: https://doi.org/10.1016/S0925-8388(99)00793-8

[24] F. Laves, H.J. Wallbaum, Zur Kristallchemie von Titan-Legierungen, Naturwissenschaften **27**, 674-675 (1939).
DOI: https://doi.org/10.1007/BF01494992

[25] Periodic Tables by Sargent-Welch Scientific Company, Sargent-Welch Scientific Company, Skokie (1980).

[26] K.R. Dhilsha, K.V.S. Rama Rao, Investigation of magnetic, magnetomechanical, and electrical properties of the $Tb_{0.27}Dy_{0.73}Fe_{2-x}Co_x$ system, J. Appl. Phys. **73** 1380-1385 (1993).
DOI: https://doi.org/10.1063/1.353258

[27] L. Sandlund, M. Fahlander, T. Cedell, A. E. Clark, J. B. Restorff, M. Wun-Fogle, elastic moduli, and coupling factors of composite Terfenol-D, J. Appl. Phys., Magnetostriction, **75**, 5656-5658 (1994). DOI: https://doi.org/10.1063/1.355627

[28] J.M.D. Coey, Magnetism and Magnetic Materials, Cambridge Univ. Press, New York (2010).
DOI: https://doi.org/10.1017/CBO9780511845000

[29] D.C. Jiles, Recent advances and future directions in magnetic materials, Acta Mater. **51**, 5907-5939 (2003).
DOI: https://doi.org/10.1016/j.actamat.2003.08.011

[30] P. Chaddah, First Order Phase Transitions of Magnetic Materials. Broad and Interrupted Transitions, CRC Press, Boca Raton (2017).
DOI: https://doi.org/10.1201/9781315155883